



## **In-depth wood temperature measurement using embedded thin wire thermocouples in cone calorimeter tests**

Lucas Terrei, Zoubir Acem, Véronique Marchetti, Paul Lardet, Pascal Boulet, Gilles Parent

### **► To cite this version:**

Lucas Terrei, Zoubir Acem, Véronique Marchetti, Paul Lardet, Pascal Boulet, et al.. In-depth wood temperature measurement using embedded thin wire thermocouples in cone calorimeter tests. *International Journal of Thermal Sciences*, 2021, 162, pp.106686. <10.1016/j.ijthermalsci.2020.106686>. <hal-04455046>

**HAL Id: hal-04455046**

**<https://hal.science/hal-04455046v1>**

Submitted on 14 Feb 2024

**HAL** is a multi-disciplinary open access archive for the deposit and dissemination of scientific research documents, whether they are published or not. The documents may come from teaching and research institutions in France or abroad, or from public or private research centers.

L'archive ouverte pluridisciplinaire **HAL**, est destinée au dépôt et à la diffusion de documents scientifiques de niveau recherche, publiés ou non, émanant des établissements d'enseignement et de recherche français ou étrangers, des laboratoires publics ou privés.



HAL Authorization

# In-depth wood temperature measurement using embedded thin wire thermocouples in cone calorimeter tests

Lucas TERREI<sup>a</sup>, Zoubir ACEM<sup>a</sup>, Véronique MARCHETTI<sup>b</sup>, Paul LARDET<sup>b</sup>, Pascal BOULET<sup>a</sup>, Gilles PARENT<sup>a</sup>

<sup>a</sup> *Université de Lorraine, CNRS, LEMTA, F-54000 Nancy, France*

<sup>b</sup> *Université Paris-Est, Centre Scientifique et Technique du Bâtiment (CSTB), France*

---

## Abstract

In-depth temperature measurements of wood samples using thermocouples are commonly performed in fire research at all scales. However, the size or the type of thermocouples or how they are placed in the sample can lead to the measured temperature being significantly different. In this work, an original method combining thin wire thermocouples with a meticulous implantation, was used to provide an accurate measurement of the in-depth temperature of wood samples during their degradation. Wood samples were thus equipped with both embedded thin wire thermocouples (0.1 mm diameter) and sheathed thermocouples (1 mm diameter) installed perpendicularly or in parallel to the conductive heat flux to compare the results between the two kinds of measurements. Afterwards, samples were exposed to the cone calorimeter at different heat fluxes (from 16.5 to 93.5 kW.m<sup>-2</sup>) in order to measure both in-depth temperature and mass loss during the degradation. The smallness and high flexibility of thin embedded wire thermocouples enabled in-depth temperature measurement without affecting the mass loss measurement. This is usually not possible when using sheathed thermocouples, because of their high stiffness. Results showed that it is crucial to rigorously control the thermocouple implantation, as an underestimation up to 400 °C was observed for thermocouples put near the surface exposed to the heat flux. There are several reasons for this difference: the heat sink due to conductive heat flux through the thermocouple body, a poor contact between the sensor and the sample and uncertainty about the actual position of the thermocouple. The char front evolution deduced from temperature measurement by wire thermocouples was found to comply with direct measurements of the char layer performed on samples. Finally, the charring rate obtained from in-depth temperature as a function of the heat flux was found to follow an affine law.

**Keywords:** Temperature measurement, cone calorimeter, mass loss rate, wood degradation, wood charring

---

## 1. INTRODUCTION

Wood materials such as cross-laminated timber (CLT), glued laminated timber (glulam) or laminated bamboo, to cite just a few, are increasingly popular for use as structural materials in buildings because of their low carbon footprint. These materials also have good mechanical properties and are convenient to machine, shape and implement in constructions. For all these reasons, wood-based materials are now increasingly used in building facades and structures. However, this combustible material degrades in a fire situation. Consequently, a good understanding of wood

17 fire resistance is important to correctly size wood structures in buildings, for reasons of fire safety  
 18 and prevention. This sizing mainly requires knowledge of the extent to which wood materials can  
 19 withstand fire and how they degrade in fire situations. Previous studies on the wood degradation  
 20 process showed a complex coupling between chemical, thermal and mechanical reactions [1, 2].  
 21 Thus, reliable in-depth temperature data are important for the development of models whose aim  
 22 is to predict wood behavior. Among other consequences, the pyrolysis of wood results in the for-  
 23 mation of a char layer whose mechanical properties are much poorer than those of wood. On the  
 24 other hand, the char layer acts as a protective layer which slows down the in-depth degradation of  
 25 wood.

26 At a small scale, several experimental studies aiming at determining the charring rate of wood  
 27 samples have been carried out in the past. Xu *et al.* [3] exposed five wood species horizontally to  
 28 the cone calorimeter at different heat fluxes and exposure times. After cutting each sample, Xu *et al.*  
 29 *al.* measured the char layer and deduced the charring rate for different wood species. This work  
 30 showed that the increase of the charring rate according to the heat flux is related to the wood  
 31 species. Other studies have shown empirical equations describing the charring rate as a function  
 32 of the heat flux [4]. The recent state of the art report on the factors which affect the burning  
 33 behavior of wood by Bartlett *et al.* [1] showed a charring rate varying from  $0.4 \text{ mm} \cdot \text{min}^{-1}$  for  
 34 hardwood to  $0.8 \text{ mm} \cdot \text{min}^{-1}$  for softwood. The value generally used in fire science engineering is  
 35  $0.65 \text{ mm} \cdot \text{min}^{-1}$  [5, 6]. The wood density, species or heating method (a heat flux increasing over  
 36 time, constant heat flux, furnace) are parameters which affect the charring rate [7, 8]. Several  
 37 empirical models are used to determine the char rate like the nonlinear char rate model used in  
 38 engineering [9]. The charring front has also been regularly deduced from the  $300^\circ\text{C}$  isotherm  
 39 measured by thermocouples in different types of tests [1, 10, 11]. Measurement of in-depth tem-  
 40 perature has commonly been performed in cone calorimeter tests by using thermocouples [12, 13].  
 41 Some papers dating back to the 1960's recommended putting thermocouples perpendicular to the  
 42 exposed heat flux (or parallel to isotherms) [14, 15]. The present paper is devoted to wood, but  
 43 most of the observations made would apply when dealing with other low thermal conductivity  
 44 materials like concrete or polymers. For practical reasons, sheathed thermocouples are generally  
 45 placed into wood samples by drilling boreholes parallel to the heat flux, i.e. perpendicular to the  
 46 exposed wood surface. However, it is difficult to make long holes with a small diameter in the  
 47 wood. Therefore, drilling is generally carried out using a drill bit with a diameter in the mil-  
 48 limeter range and the thermocouples put into the material are also millimeter-sized. Also, when  
 49 using sheathed thermocouples, mass loss cannot be measured accurately because the thermocouple  
 50 stiffness affects the mass measurement. Thus, tests must be doubled in order to get the in-depth  
 51 temperature and the mass loss rate, but not simultaneously [16]. Moreover, this method can lead  
 52 to mismeasurements due to the thermal sink along the thermocouple, the inertia of the sheath,  
 53 the poor contact between the sensor and the sample or even because of the inaccurate location  
 54 of sensors. Fahrni *et al.* conducted two interesting studies related to in-depth temperature mea-  
 55 surement in wood samples [17, 18]. In these works, up to nine different combinations of types  
 56 of thermocouple/ways of setting-up were studied - sheathed or wire thermocouple, hot junction  
 57 nature (welded or twisted), thermocouple inserted in boreholes or inlaid in the sample, diameter of  
 58 the thermocouple wires, maximum diameter of the thermocouple (sheath diameter or diameter of  
 59 the wires including electrical insulation), diameter of the borehole (if applicable) and orientation  
 60 of the thermocouple. A comprehensive designation to describe all these parameters was proposed.  
 61 In reference. [17], tests were performed both inside a furnace following the ISO 834 fire exposition

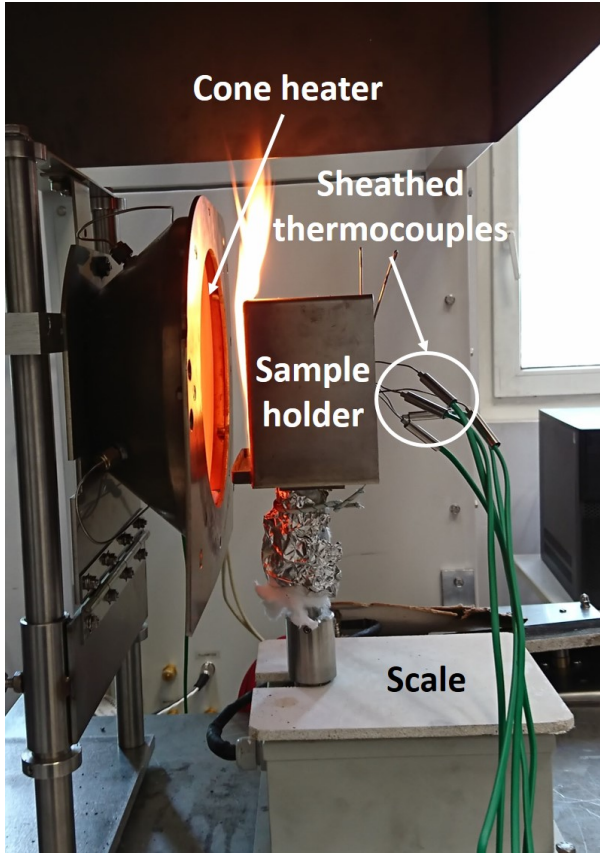
62 and by submitting the sample to a constant heat flux equal to  $55 \text{ kW.m}^{-2}$ . In reference. [18],  
 63 only the furnace was used. The main finding of these two works is that measurements can be very  
 64 different according to the design used and that discrepancies reaching several hundred degrees were  
 65 observed. The designs in which the thermocouple body (wires or sheath) is oriented parallel to  
 66 the isotherms were always found to give the highest temperature values which are undoubtedly  
 67 the most reliable. The difference was mainly attributed to heat transfer along the thermocouple  
 68 body. The secondary cause leading to the under-measurement of temperature was attributed to  
 69 the thermal contact between the thermocouple and the sample. Convection inside the borehole,  
 70 when this was significantly larger than the thermocouple, was found to be negligible. Cooling of  
 71 the thermocouple surrounding was also observed. In the present work, spruce wood samples were  
 72 exposed to different heat fluxes (16.5, 38.5, 60 and  $93.5 \text{ kW.m}^{-2}$ ) with a cone calorimeter ori-  
 73 ented vertically, in order to measure the in-depth temperature evolution. This measurement was  
 74 performed with two types of thermocouple implantations. In the first setup non-insulated very  
 75 thin wire thermocouples (0.1 mm diameter) were embedded in the sample after specific machining  
 76 aimed at controlling the position of the measurement. Such small thermocouples have the ad-  
 77 vantage of being minimally intrusive compared to the thermocouples that are usually used which  
 78 are commonly millimeter-sized. Following the designation proposed by Fahrni *et al.*, this design  
 79 would be named K-w-e-0.1/0.1/in-pa. Compared to the parallel design studied by Fahrni *et al.*,  
 80 the present one involved thinner wire diameter (0.1 mm vs 0.2 mm) and thinner maximum ther-  
 81 mocouple diameter (0.1 mm vs 1.2 mm, because of the lack of electrical insulation). The accuracy  
 82 provided by our design is thus expected to be even better, and less intrusive. In the second method,  
 83 1.2 mm diameter holes were drilled from the sample back side and 1 mm diameter sheathed ther-  
 84 mocouples were inserted inside with the depth position adjusted directly from the hole depth. The  
 85 designation of this second implantation is thus K-s-i-0.2/1/1.2-pe. The temperature evolutions  
 86 obtained with the two types of thermocouple implantation are compared each other. Afterwards,  
 87 the measured in-depth temperatures from both techniques were used in order to track the char  
 88 front position from the  $300 \text{ }^{\circ}\text{C}$  isotherm. Results were compared with direct measurements from  
 89 samples cut in their middle after being exposed to the same heat fluxes for different durations.  
 90 Finally, a study of the charring rate, calculated from the char front positions, was also performed.

## 91 2. MATERIALS AND METHODS

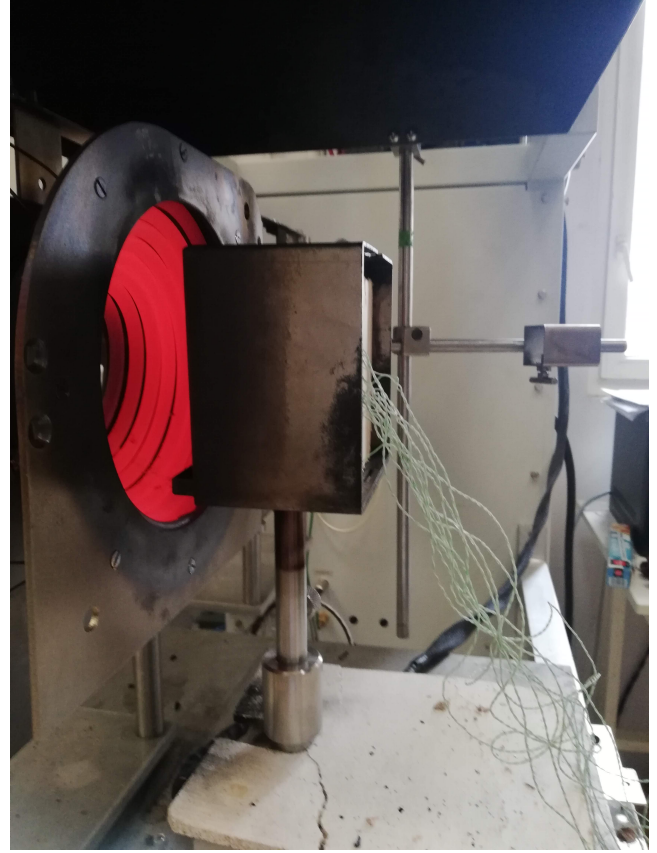
### 92 2.1. Experimental setup

93 Tests were performed with a cone calorimeter oriented vertically. Figure 1 presents the exper-  
 94 imental setup.





(a) Sample equipped with sheathed thermocouples.



(b) Sample equipped with wire thermocouples.

Figure 1: Experimental setup.

95 The experiment consists of exposing a sample to a radiative heat flux coming from an electrically  
 96 heated conical coil. The radiative heat flux emitted by the cone was measured before each test  
 97 using a Schmidt-Boelter fluxmeter (Medtherm). The heat flux was considered correct when its  
 98 value was  $\pm 0.5 \text{ kW.m}^{-2}$  from the desired flux. The distance between the sample and the heater  
 99 was 25 mm. The spark igniter was not placed between the cone and the sample so that the wood  
 100 ignition was not explicitly piloted. The selected samples were of spruce wood which were  $100 \times 100$   
 101  $\text{mm}^2$  in size with a 50 mm thickness and the heat flux was perpendicular to the wood grain.  
 102 The sample average density was about  $490 \text{ kg.m}^{-3}$  for an average moisture content around 9.5 %.  
 103 Wood samples were exposed to different constant incident heat fluxes equal to 16.5, 38.5, 60 and  
 104  $93.5 \text{ kW.m}^{-2}$ . This large range of heat fluxes made it possible to study the in-depth temperature  
 105 time evolution either with sample flaming auto-ignition (for high enough heat fluxes) or without  
 106 ignition. The experiment lasted for between 15 and 60 minutes according to the imposed heat flux.

## 107 2.2. Setting up thermocouples in the sample

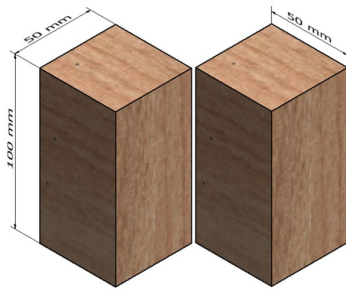
108 In-depth temperature measurements by thermocouples are commonly performed in cone calorime-  
 109 ter tests. As aforementioned, the type of thermocouples used and the way they are implemented  
 110 can greatly affect the measured in-depth temperature. In this work, a method was developed  
 111 aiming at embedding very thin (0.1 mm diameter) wire thermocouples inside the sample. Eleven  
 112 K-type thermocouples were placed inside the wood sample. Figure 2 shows the meticulous ma-

chining steps used for embedding wire thermocouples in the sample. There are four main steps to the proposed protocol:

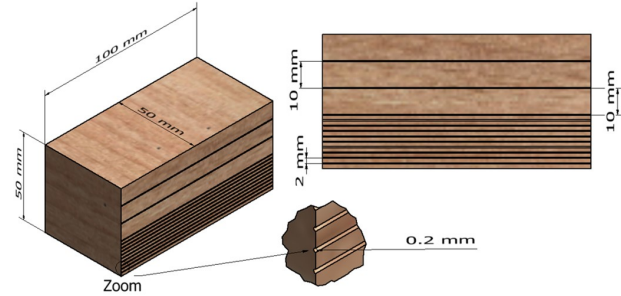
- Step 1: The sample was cut in the middle, perpendicularly to the exposed surface.
- Step 2: 0.2 mm depth and width square-grooves were precisely machined (with a 0.2 mm thickness circular milling cutter) on the surface of the wood at the desired locations (every 2 mm from 2 to 20 mm depth from the exposed surface, one at a 30 mm depth and a last one at a 40 mm depth).
- Step 3: After machining, wire thermocouples were put in the square-grooves. In this picture red dots represent the position of the thermocouple junction which was homemade welded where the temperature is measured. The alumel and chromel cables were welded by autogenous electric welding (without adding metal) end to end.
- Step 4: Samples were finally glued with Melamine-urea-formaldehyde (MUF) and pressed for 6 hours.

Setting up wire thermocouples in this way takes three hours per sample from grooving to bonding and including thermocouple welding. This process can be carried out on a larger scale, but it becomes more difficult the more the sample size increases. For example, it was also used by the authors for Single Burning Item (SBI) tests with samples as large as  $150 \times 50$  cm.

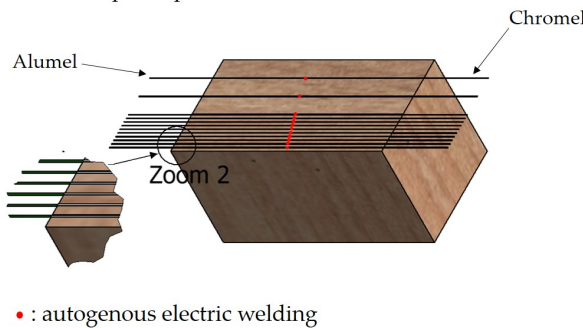
Step 1: Sample cut in half



Step 2 : Square-grooves machining



Step 3: Thermocouple implantation



Step 4: Sample glued and pressed

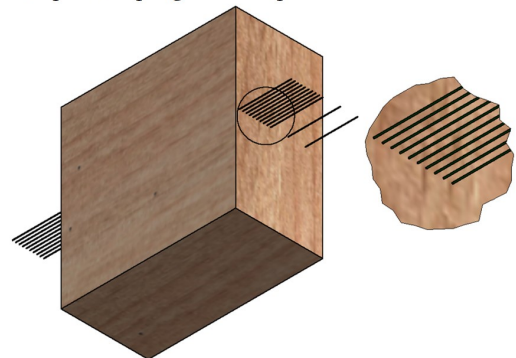


Figure 2: Wire thermocouple implantation in wood sample: main steps of the setting-up.

130 The first experiment consisted of checking if the process could have modified the sample and  
 131 also if the mass loss of the sample can be reliably measured with the wire thermocouples installed  
 132 inside. For that purpose, mass loss measurements were performed with a virgin sample and with  
 133 a sample fitted with thin wire thermocouples. The heat flux was set at  $60 \text{ kW.m}^{-2}$  and the test  
 134 duration 15 minutes. The results are shown in figure 3.

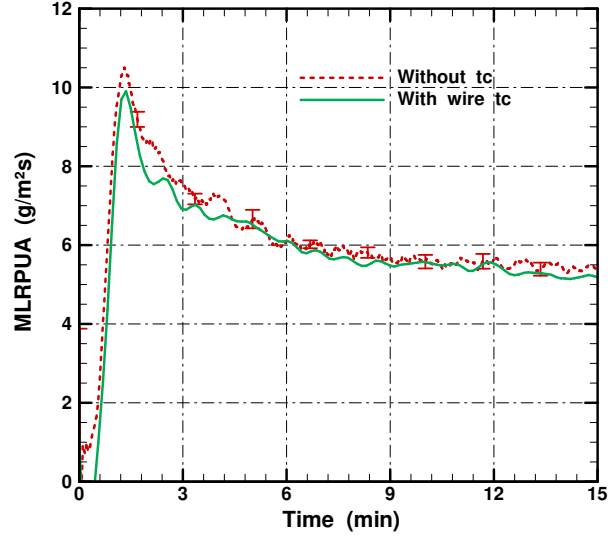


Figure 3: MLR for tests with and without embedded wire thermocouples. Heat flux  $60 \text{ kW.m}^{-2}$ .

135 It appears that MLR evolutions are very similar. Tests with embedded wire thermocouples  
 136 can be thus considered to be carried out in similar conditions as without. Compared to existing  
 137 ways of proceeding, the thermocouple implantation proposed in the present paper has numerous  
 138 advantages for achieving more accurate and reliable in-depth temperature measurements namely:

- 139 - The thermocouple wires are very thin which minimizes the conductive heat flux along them  
 140 and the intrusiveness of the wires in the sample (very tiny matter removal, very low quantity  
 141 of glue).
- 142 - The wires are very supple which means that mass loss measurements can be performed at  
 143 the same time as temperature measurements.
- 144 - The chromel and alumel wires extend from each other in one straight unit and therefore no  
 145 electrical insulation is required. These two points mean that thinner grooves can be used to  
 146 put them inside the wood
- 147 - The autogenous electric welding is very small (no additional matter).
- 148 - The position of the thermocouple junction is very accurate.
- 149 - The thermal resistance between the thermocouple and the sample is negligible.
- 150 - The wires are parallel to the isotherms thus minimizing the conductive flux as will be shown  
 151 later and this is undoubtedly the main positive point of this method.

### 152 3. RESULTS AND DISCUSSION

153 Results and discussion are dissociated in three parts. The first part presents in-depth temper-  
154 atures measured by embedded wire thermocouples at different heat fluxes. The second section is  
155 devoted to a comparison with the other kind of thermocouple implantation. A numerical simula-  
156 tion was performed showing that the conductive heat flux through the thermocouple can actually  
157 lead to very large mismeasurements. Finally, the 300 °C isotherm deduced from temperature  
158 measurements are compared with the directly measured charring rate.

#### 159 3.1. In-depth temperature measured by thin embedded wire thermocouples

##### 160 3.1.1. Thermograms

161 The wood samples equipped with embedded wire thermocouples were exposed to the cone  
162 calorimeter at several heat fluxes from 16.5 to 93.5 kW.m<sup>-2</sup>. Results obtained for tests performed  
163 at 16.5, 38.5, 60 and 93.5 kW.m<sup>-2</sup> are presented in figures 4 to 7. In figures 4 and 6, surface  
164 temperature is added to in-depth thermograms. This temperature was measured with an infrared  
165 camera equipped with a filter at 3.9 μm wavelength (outside emission bands of combustion gases).  
166 At the cone calorimeter scale and especially with a vertical orientation, the optical thickness of the  
167 flame is small enough to consider that there is a low level of emission by soot and consequently  
168 to assume that the flame is almost transparent outside gas emission bands [19]. The surface  
169 temperature measurements are described with more details in [20]. As a general observation, the  
170 consecutive in-depth temperature curves are ordered according to the thermocouple depth and  
171 their spacing is rather regular. The surface temperature curve is higher than in-depth temperature  
172 curves and its variation is consistent with in-depth curves. In particular there is no odd gap between  
173 surface temperature and 2 mm in-depth temperature. The profile temperature curves presented in  
174 figure 7 were also found to have very likely behavior with no spurious steps or slope changes which  
175 made us very confident about the quality of the performed measurements. As the exposure time  
176 increases, some measured in-depth temperatures become noisy and somewhat erratic, sometimes  
177 exceeding the surface temperature. This happens when the thermocouple is no longer embedded  
178 inside the sample, due to the char combustion and thus the thermocouple is directly submitted to  
179 the flux from the heater and to the flame turbulent hot gases.

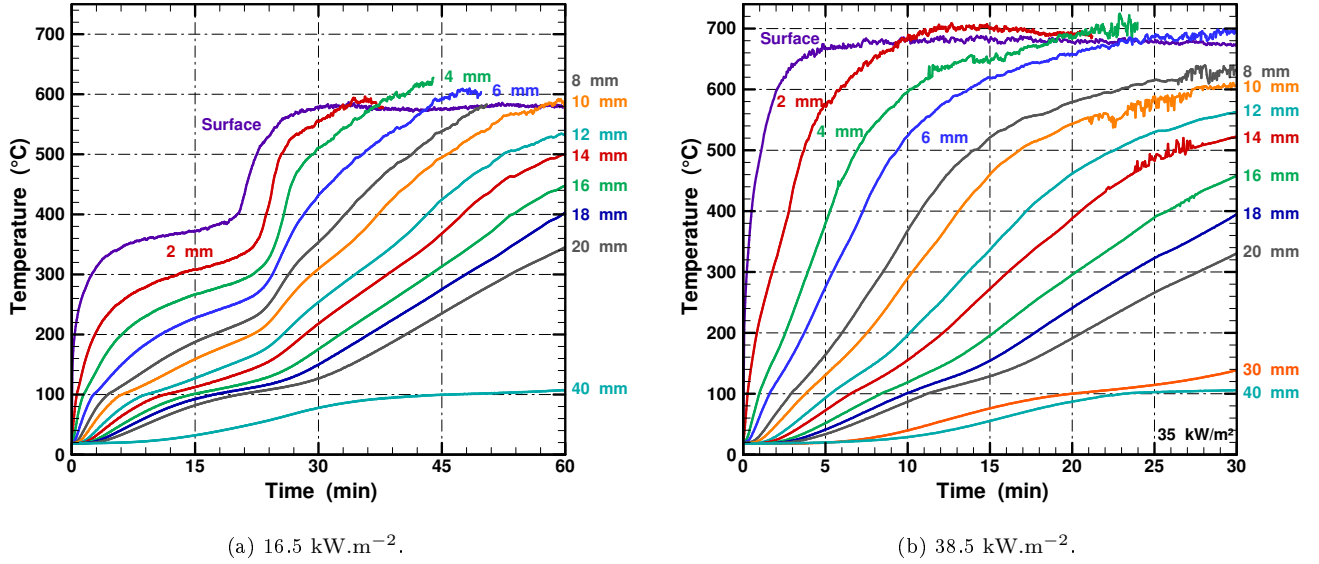


Figure 4: In-depth temperature evolutions measured by embedded wire thermocouples located from 2 to 40 mm depth to the exposed surface.

180 The results obtained for tests performed at  $16.5 \text{ kW.m}^{-2}$  and  $38.5 \text{ kW.m}^{-2}$  are presented in figure 4.  
 181 For these two low heat fluxes auto-ignition did not occur. For the test performed at  $16.5 \text{ kW.m}^{-2}$ ,  
 182 surface temperature first increases fast and asymptotically tends toward a first plateau at around  
 183  $400 \text{ }^{\circ}\text{C}$  or little below. However, at a time equal to 20 minutes, the temperature rises fast again  
 184 before reaching a new equilibrium temperature near  $580 \text{ }^{\circ}\text{C}$ . This change in behavior is due  
 185 to the smouldering combustion of char beginning which brings an additional heat source. This  
 186 transition was already noticed in papers devoted to the study of the surface temperature of wood  
 187 samples in cone calorimeter tests [20, 21]. Figure 5 shows infrared pictures taken at different  
 188 times during a test performed at a  $16.5 \text{ kW.m}^{-2}$  heat flux. These pictures show the smouldering  
 189 combustion onset at 20 minutes (picture 2). The beginning of the smouldering combustion results  
 190 in glowing hot zones (pink color areas in the snapshot) which then spread over the entire surface.  
 191 The influence of char combustion can also be seen in depth particularly for depths less than or  
 192 equal to 6 mm. The beginning of the second temperature rise is delayed compared to the surface  
 193 temperature, and, logically, the deeper the position, the larger this delay. The new equilibrium  
 194 temperature is also lower when the depth increases. For depths greater than 6 mm, the “effect”  
 195 of char combustion becomes less and less remarkable, since thermocouples are either far from the  
 196 regressive smouldering surface or even from the charring front. For the test performed at  $38.5$   
 197  $\text{ kW.m}^{-2}$ , there is no flame ignition either. Smouldering combustion occurred too but at a shorter  
 198 time for which temperature increases still fast, so its influence is not so obvious. The maximum  
 199 temperature reached at 40 mm depth is around  $100 \text{ }^{\circ}\text{C}$  for  $16.5 \text{ kW.m}^{-2}$  and  $250 \text{ }^{\circ}\text{C}$  for  $38.5$   
 200  $\text{ kW.m}^{-2}$  after one hour of exposure.

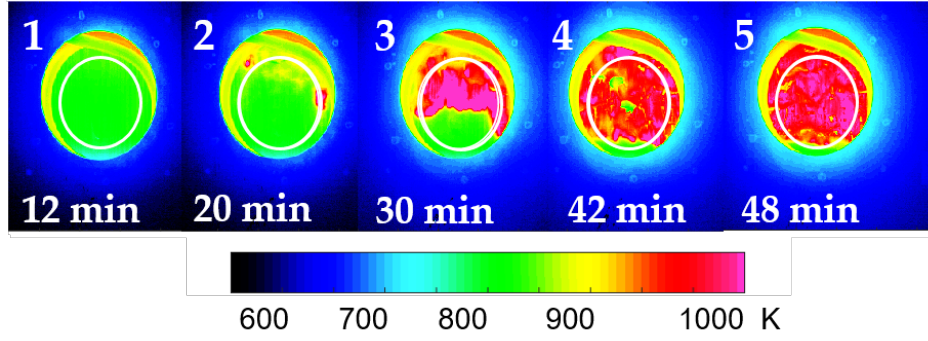


Figure 5: Surface temperature field in Kelvin and studied area (white circle) at different exposure time for  $16.5 \text{ kW.m}^{-2}$ .

Figure 6 presents typical in-depth temperature evolutions for tests at 60 and  $93.5 \text{ kW.m}^{-2}$ , for which wood auto-ignition occurred. For the heat flux equal to  $60 \text{ kW.m}^{-2}$  three tests were performed and errors bars correspond to standard variations.

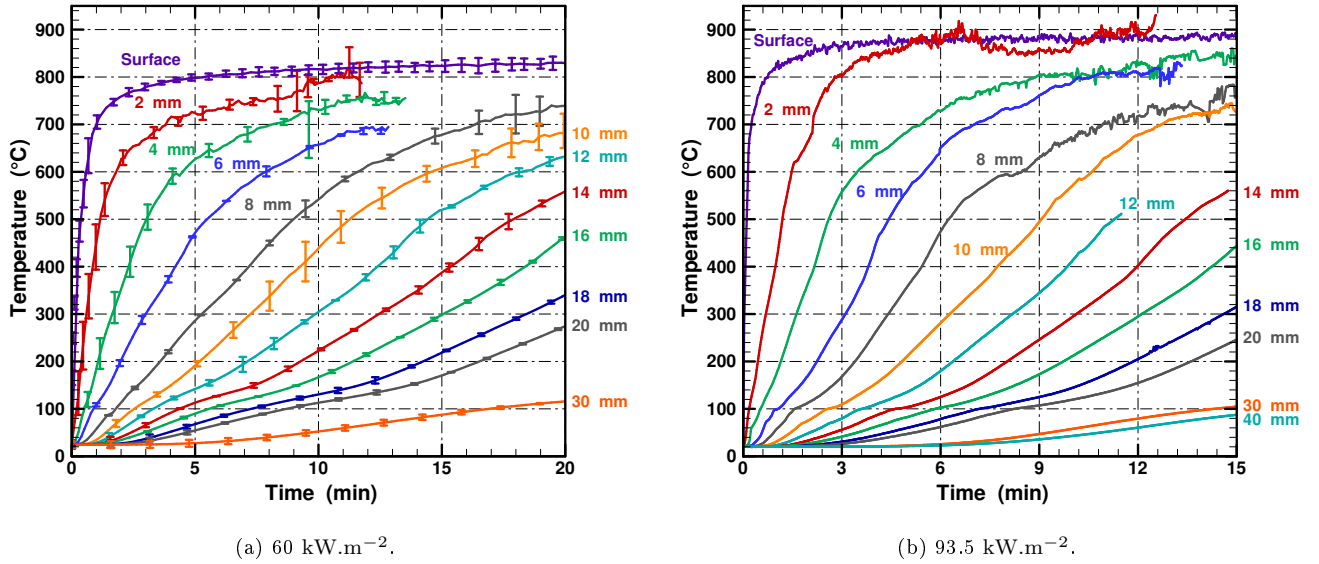


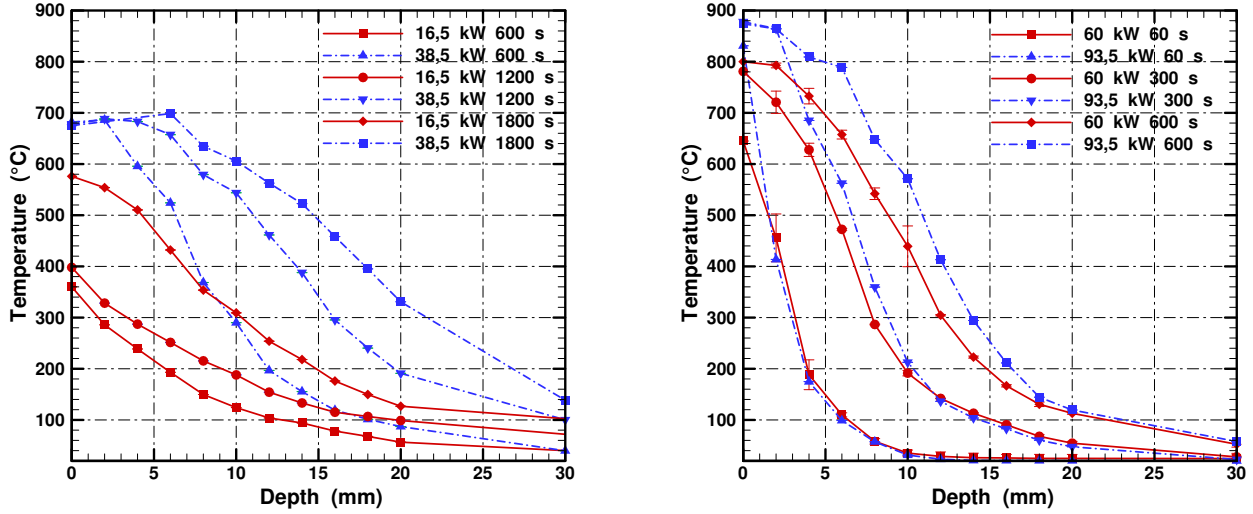
Figure 6: In-depth temperature evolutions measured by embedded wire thermocouples from 2 to 40 mm depth to the exposed surface.

Surface temperature reaches a plateau fast and, the higher the heat flux, the higher this value is logically. As a consequence of the low thermal diffusion of the sample, the larger the depth, the lower the plateau value and the later the plateau occurs. The higher the heat flux, the faster the temperature rises in the wood. For instance, the temperature at 18 mm depth reaches  $300^\circ\text{C}$  in 18 min 30 sec for a  $60 \text{ kW.m}^{-2}$  incident heat flux, whereas it takes only 14 minutes for a  $93.5 \text{ kW.m}^{-2}$  incident heat flux. In the case of thermocouples close to the surface exposed to the heat flux, the temperature increases rapidly followed by a plateau. The temperature of thermocouples close to the exposed surface (from 2 to 6 mm depth) increases fast at the beginning of the test.

At 2 mm depth, the temperature reaches 600 °C in 107 and 88 seconds for 60 and 93.5 kW.m<sup>-2</sup> respectively. For large depths (10 mm and above), there is a delay before the temperature begins to rise. Then, the temperature increase slows down. When the temperature reaches around 150 °C the slope increases again.

### 3.1.2. Temperature profiles

In-depth temperature measurement provided by embedded thermocouples were used to draw temperature profiles within the sample. Results for different heat fluxes and at different times are presented in figure 7.



(a) 16.5 and 38.5 kW.m<sup>-2</sup> at 600, 1200 and 1800 sec.

(b) 60 and 93.5 kW.m<sup>-2</sup> at 60, 300 and 600 sec.

Figure 7: Temperature profiles at different times and different heat fluxes.

In figure 7a, the temperature profiles within the sample are logically higher for 38.5 kW.m<sup>-2</sup> than for 16.5 kW.m<sup>-2</sup>. At 10 mm depth, 600 °C are reached after 30 minutes of exposure to 38.5 kW.m<sup>-2</sup> while the measured temperature is 300 °C at the same depth for 16.5 kW.m<sup>-2</sup>. The smouldering combustion considerably increases the in-depth temperature. In figure 7b, at the beginning of the test for 60 kW.m<sup>-2</sup>, a larger dispersion ( $\pm 85$  °C) is observed for the temperature at 2 mm depth due to the fast heating dynamics. The in-depth temperatures close to the exposed surface rises quickly to reach a maximum value close to the temperature of cone coils. At a same time, the temperature close to the exposed surface is logically higher for tests at 93.5 kW.m<sup>-2</sup> than for the tests at 60 kW.m<sup>-2</sup>. The heat is then transferred by conduction within the sample resulting in a progressive growth of temperature. It should be reiterated that during the experiments, as samples degrade and crack, the first wire thermocouples were no longer embedded in the wood and were directly exposed to cone calorimeter. When this occurred, the measured temperature becomes unstable and the values can no longer be considered reliable.

### 3.2. Influence of the thermocouple setting-up on in-depth temperature measurements

Some tests were also performed with 1 mm-diameter thermocouples placed perpendicularly to isotherms after drilling the back of the sample. This kind of implantation is typically employed



in most fire science experiments since it is quite convenient to setup. One millimeter diameter thermocouples are the standard thermocouple size. Smaller diameter sheathed thermocouple are available but they are more fragile and larger diameter holes would need to be drilled in any case because smaller drill bits are not strong enough to be used. The aim of this part of the study was to assess discrepancies which could arise in measurements carried out with the usual thermocouple implementation. In the following “wire thermocouples” will denote the thin wire thermocouples embedded inside the sample parallel to the surface exposed to the heat flux, as presented in this paper. “Sheathed thermocouple” will denote the 1 mm diameter sheathed thermocouples put inside the sample perpendicular to the surface exposed to the heat flux. The differences between the two types of measurements can be attributed at first sight to both the difference in diameter and the difference in orientation. A COMSOL simulation will allow the respective importance of these two parameters to be assessed.

### 3.2.1. Experimental study

Four sheathed K-type thermocouples (1 mm diameter) were placed respectively at 2, 4, 6 and 8 mm depth of the exposed surface. The position of the sheathed thermocouples is shown in figure 1. These thermocouples were placed perpendicularly to the surface exposed to the heat flux after drilling the back of the sample. As suggested by Reszka *et al.* [16], sheathed thermocouples were spaced by 20 mm in order to limit mutual disturbance Figure 8 presents results obtained for heat fluxes equal to  $16.5 \text{ kW.m}^{-2}$  and  $38.5 \text{ kW.m}^{-2}$ .

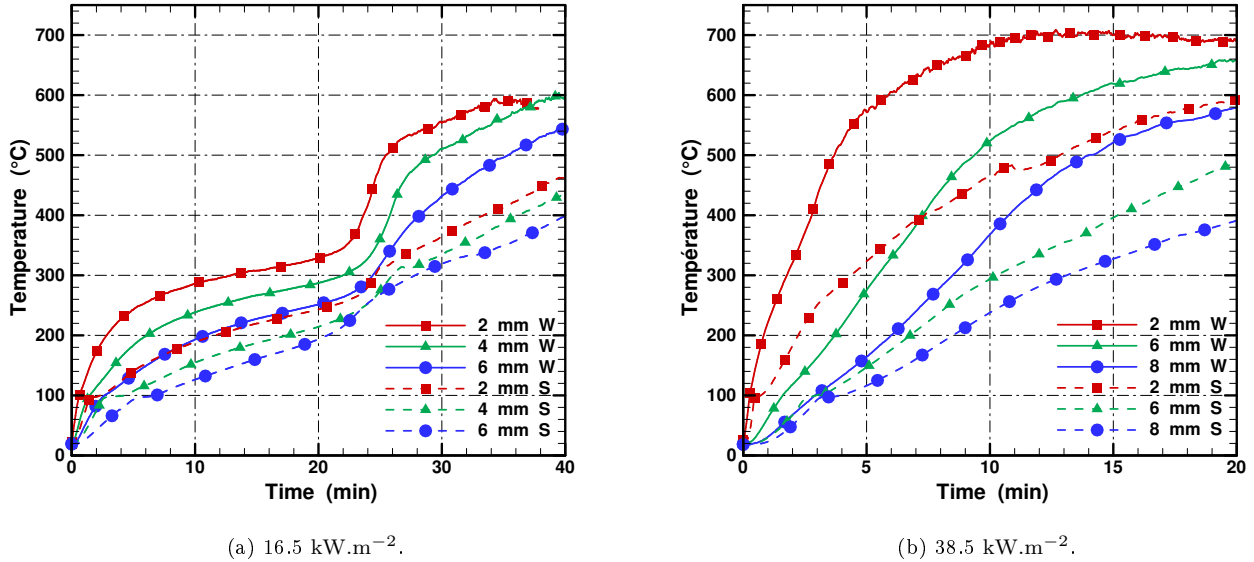


Figure 8: Mean in-depth temperature evolution for tests performed with sheathed (S) and wire (W) thermocouples.

It should be noted that the temperature evolutions for the two types of thermocouple are very different. For tests performed at  $16.5 \text{ kW.m}^{-2}$ , discrepancies reaching  $100 \text{ }^{\circ}\text{C}$  or more can be observed between the temperature measured by the two kinds of thermocouples. The beginning of smouldering combustion is observed for both techniques but it is not so clear with the sheathed thermocouples. For tests carried out at  $38.5 \text{ kW.m}^{-2}$ , the temperature measured by the sheathed



thermocouples are still largely underestimated and the difference can reach more than 200 °C. The difference between the two kinds of measurements can mainly be explained by the large heat sink through the thermocouple sheath. Indeed, the sheathed thermocouple has a high conductivity and large diameter. This means there is a large conductive heat flux along the thermocouple whereas the heat brought to the thermocouple apex is weak due to the low conductivity of wood (or of char) and the poor thermal contact between the thermocouple and the sample.

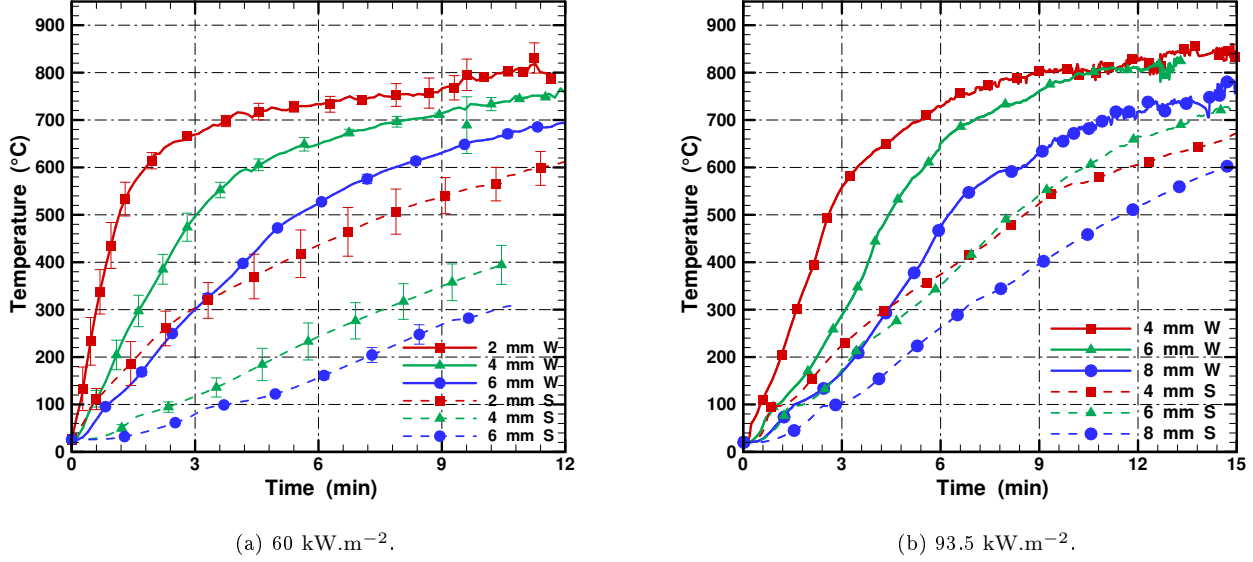


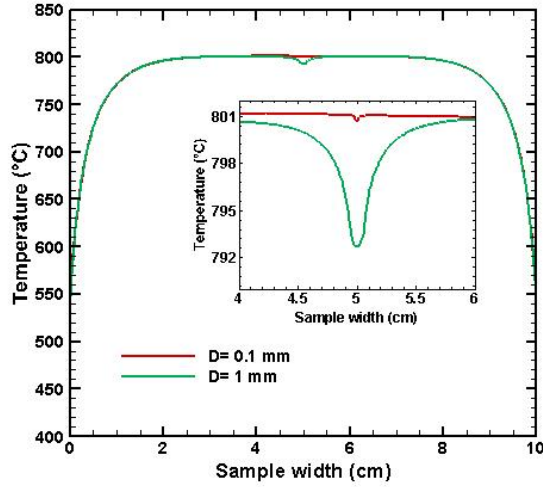
Figure 9: Mean in-depth temperature evolution for tests performed with sheathed (S) and wire (W) thermocouples.

Figure 9 presents results obtained at higher fluxes equal to 60 and 93.5 kW.m<sup>-2</sup>. Three tests were carried out at 60 kW.m<sup>-2</sup> and figure 9a shows the mean temperature obtained from these three tests with error bars corresponding to the standard deviation between the tests. Once again, the temperature evolutions for the tests performed at 60 and 93.5 kW.m<sup>-2</sup> are underestimated with sheathed thermocouples for the same reasons as for lower heat fluxes. Temperatures obtained from wire thermocouples increase fast before reaching a plateau whereas temperature evolutions provided by sheathed thermocouples are more linear and gradual. Temperature differences between the measurements made by the two thermocouple setups can reach several hundreds of degrees which is considerable. For the two heat fluxes, the temperature discrepancy reaches up to 400 °C at the beginning of the test, during the fast increase of temperature. After 9 minutes of exposure, the deviation is about 200 °C, which is still very high. Moreover, error bars for curves obtained by sheathed thermocouples are larger than those corresponding to wire thermocouple measurements. This is evidence of the inferior level of repeatability of measurements performed by sheathed thermocouples. This can be explained by larger sources of inaccuracy, including: exact position of the thermocouple (drilling process), thermal resistance between the thermocouple and the wood, the hole having to be larger than the thermocouple, etc. As a consequence, a large underestimation of the temperature is observed (which will be illustrated in next section with a COMSOL multiphysics® simulation). Furthermore, the position of sheathed thermocouples can be inaccurate particularly if these are perpendicular to the heat flux for the purposes of the study.

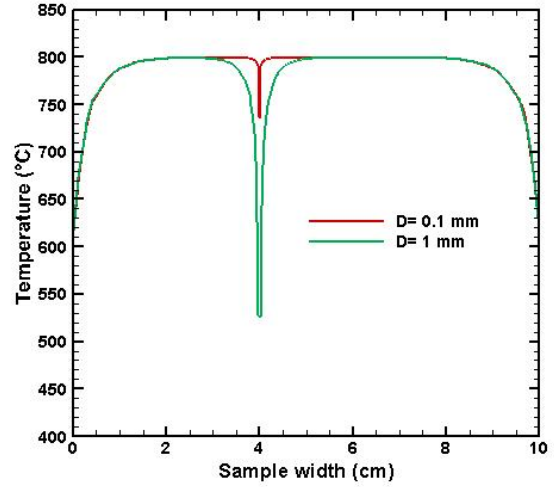
Indeed, the long and thin drill bits (typically 1.2 mm diameter and several dozens of millimeters of drilling depth) get bent easily when encountering timber heterogeneities (e.g. knots or growth rings) during the drilling process. Embedded wire thermocouples thus appear preferable to achieve accurate in-depth temperature measurements. Moreover, thanks to their high flexibility, such fine wire thermocouples allow MLR measurement during tests, which is not possible with the usual large diameter sheathed thermocouples.

### 3.2.2. *Simulation of the heat sink created by the thermocouple implantation*

Simple simulations with COMSOL multiphysics® software were performed in order to illustrate the effect of a thermocouple implantation in a wood sample. The aim was to demonstrate that the perturbation created by inserting a material having a high conductivity in a low conductivity material can be very significant rather than to actually present a predictive model providing an accurate temperature evolution. For that purpose, the sample was modelled to the cone test dimensions (*i.e.*  $100 \times 100 \times 50$  mm) and a thermocouple was placed at 2 mm away from the exposed surface. The sample mesh for the two thermocouple orientations is shown in Fig. A.15 in appendix. The mesh has 24,000 nodes for the configuration where the thermocouple is perpendicular to the surface exposed to the flow and 20,000 nodes when the thermocouple is oriented parallel to the surface. The sample was considered inert, which means that the heat transfer inside it is purely diffusive. Temperature at a large time interval (10 minutes) was considered so that the char depth is higher than 2 mm where the thermocouple junction is placed. The sample density and thermal properties were then chosen to be equal to the char properties -  $135 \text{ kg.m}^{-3}$  for the density,  $1650 \text{ J.kg}^{-1}.\text{K}^{-1}$  for the specific heat and  $0.073 \text{ W.m}^{-1}.\text{K}^{-1}$  for the conductivity. The thermocouple was modelled as a homogeneous cylinder of inconel having a density, a specific heat and a thermal conductivity equal to  $8250 \text{ kg.m}^{-3}$ ,  $444 \text{ J.kg}^{-1}.\text{K}^{-1}$  and  $14.8 \text{ W.m}^{-1}.\text{K}^{-1}$  respectively. Two orientations were considered namely parallel or perpendicular to the heat flux. For the parallel configuration, the thermocouple was put at the center of the back of the sample and its apex set at a distance equal to 2 mm from the front surface. Two diameters (1 mm and 0.1 mm ) were considered. For the perpendicular configuration, the thermocouple was set perpendicular to one of the side faces, at the middle of its width and 2 mm from the exposed surface. A perfect thermal contact between the thermocouple and the wood was assumed. A convective exchange coefficient was considered on all non-exposed surfaces equal to  $10 \text{ W.m}^{-2}.\text{K}^{-1}$  and  $15 \text{ W.m}^{-2}.\text{K}^{-1}$  on the exposed surface to the heat flux [22, 23]. An imposed radiative heat flux of  $93.5 \text{ kW.m}^{-2}$  was applied to the exposed surface. The temperature profile within the sample width 2 mm depth is presented in figure 10 for each configuration at time  $t = 600 \text{ s}$ .



(a) Parallel to the heat flux.



(b) Perpendicular to the heat flux.

Figure 10: Temperature profiles in the sample along a line passing through the thermocouple apex (2 mm depth) - Two diameters (0.1 and 1 mm) and two orientations relative to the heat flux.

At a same depth, a large drop can be observed between the temperature at the thermocouple location and the temperature far from the thermocouple. This drop reaches 280 °C which is in the same order of magnitude to what is observed experimentally. This large difference is due to the conductive heat flux along the thermocouple sheath. Moreover, the temperature drop extends for several millimeter inside the sample itself, confirming the cooling of the thermocouple surrounding noticed by Fahrni *et al.* [17] for instance. If we consider a 0.1 mm diameter thermocouple parallel to the conductive heat flux, the temperature underestimation is now only 60 °C because the conductive heat flux along the thermocouple is considerably less due to its smaller section. For the thermocouple implemented perpendicular to the heat flux, the underestimation is equal to 8 °C for a 1 mm diameter thermocouple and only 0.3 °C for a 0.1 mm diameter thermocouple (this case corresponding to the thin embedded wire thermocouple used in the present work). Although this simulation was not intended to be quantitative because a lot of phenomena were not taken into account (pyrolysis, change of thermal properties of materials, thermal contact resistance and so on), it does demonstrates that very large temperature differences can be observed depending on the thermocouple size and the way it is implanted inside the sample. The thermocouple orientation is found to be the most influential parameter because the conductive heat flux along the thermocouple wire (or sheath) is proportional to the temperature gradient. Even with a large diameter thermocouple, the temperature underestimation is only 8 °C when it is oriented perpendicular to the heat flux. For a given orientation, the larger the thermocouple diameter, the larger the conductive heat flux and thus the temperature underestimation. Almost negligible temperature difference is obtained using a very thin thermocouple oriented perpendicular to the heat flux. Adding a thermal resistance between the sample and the thermocouple would result in an even higher underestimation of the temperature.

### 3.3. Comparison between 300 °C isotherm and char front

It is often reported that the progress of the char front within the sample follows the 300 °C isotherm [24]. Thus, the new thermocouple implantation was used to study the char layer progression in the sample. To validate this approach, the position of the char front was also determined directly - wood samples were submitted to a given heat flux (60 and 93.5 kW.m<sup>-2</sup>) for different durations and then cooled fast with liquid nitrogen to stop pyrolysis reactions. These samples were cut in their middle and the position of the char front was measured with a rule. In figure 11, this char front position is compared to the one obtained indirectly from the position of the 300 °C isotherm. The error bars for the char front deduced from thermocouples (wire and sheathed) correspond to the standard variations obtained from three tests for each heat flux.

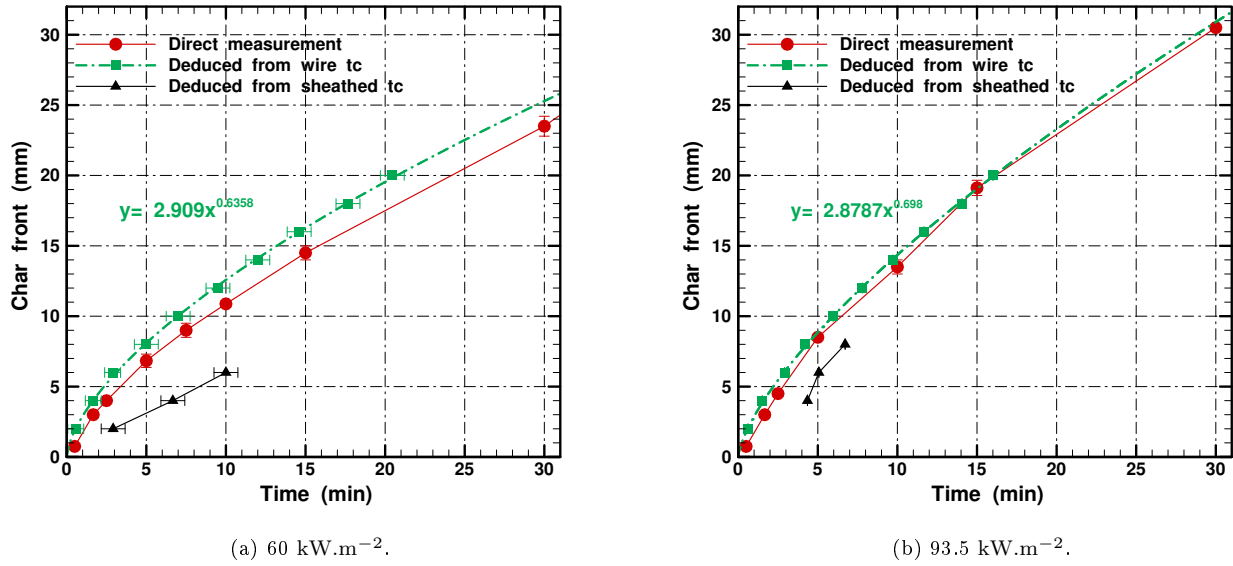
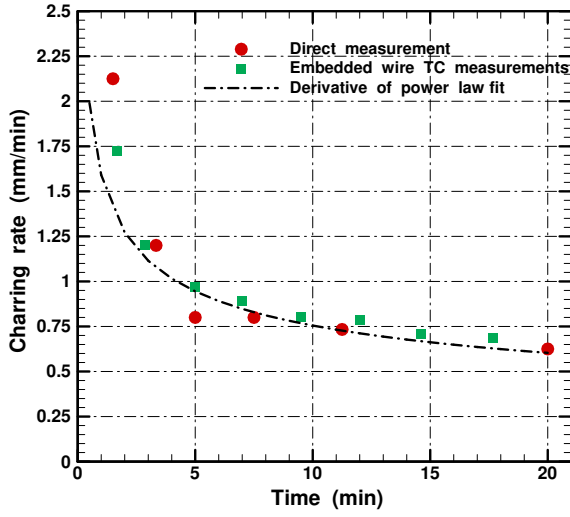
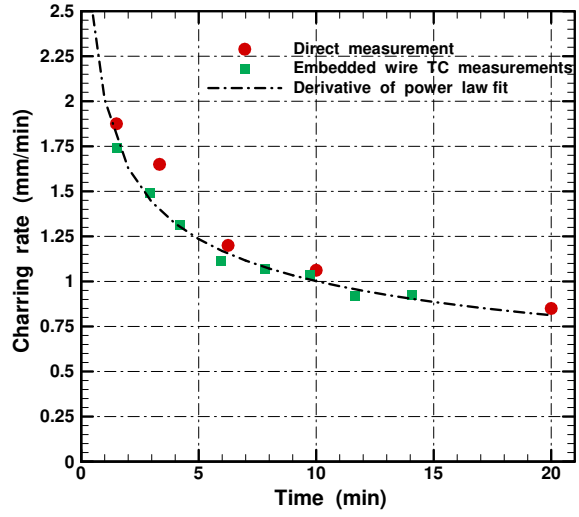


Figure 11: Char front positions measured with a rule and deduced from the 300 °C isotherm provided by sheathed and wire thermocouples. For measurement marks having error bars, three measurements were performed and error bars correspond to standard variations. For single marks, only one measurement was performed.

Figure 11 shows a good level of compliance between direct measurements of the char front position and the position obtained from the 300 °C isotherm measured with the embedded wire thermocouples. This means we can have even more confidence about the accuracy of the measurements that were made in this way. By contrast, when considering the 300 °C isotherm measured with sheathed thermocouple, a large discrepancy can be noticed. For instance, for a test performed at 60 kW.m<sup>-2</sup>, the char front is located at a 6 mm depth after 180 seconds according to embedded wire thermocouple measurements while 620 seconds are needed when considering sheathed thermocouple data. A power fit was performed on wire thermocouple measurements. It can be seen that the power law fits pretty well with the data and this kind of fit makes it possible to calculate an analytical charring rate. Figure 12 presents the charring rate deduced from the char front position. The charring rate for wire thermocouples was deduced with centered finite differences for values calculated from measured data (green squares) and with analytical derivative of the power law (dot-dashed curve).



(a) 60 kW.m<sup>-2</sup>.



(b) 93.5 kW.m<sup>-2</sup>.

Figure 12: Charring rates deduced from the char front measured with a rule and deduced from with the 300 °C isotherm of wire thermocouples.

The charring rate evolutions deduced from rule measurements and wire thermocouples isotherm comply well with the two heat fluxes. Using the position of the 300 °C isotherm, measured by the embedded thermocouples, makes it possible to obtain the char front position and the charring rate from a single test, which is not possible using the direct method which provides only discrete values with each value coming from a different test. The charring rate was found to reach a peak value around 2.5 mm.min<sup>-1</sup> in a transient part and to decrease to a quasi-steady state around 0.8 mm.min<sup>-1</sup>. In the following, the variation of the charring rate with the submitted heat flux was also investigated.

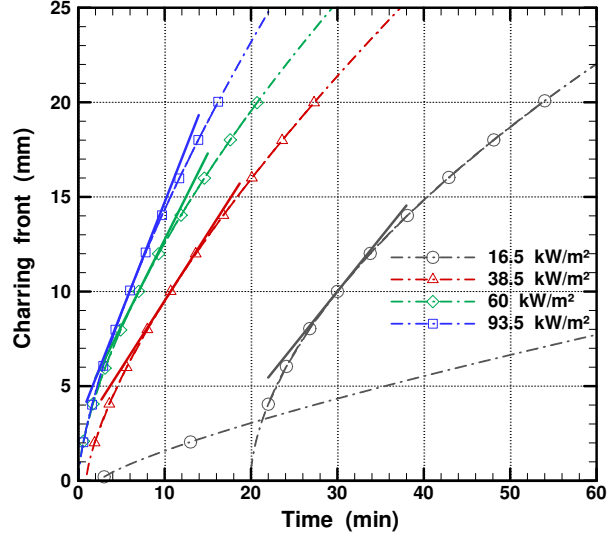
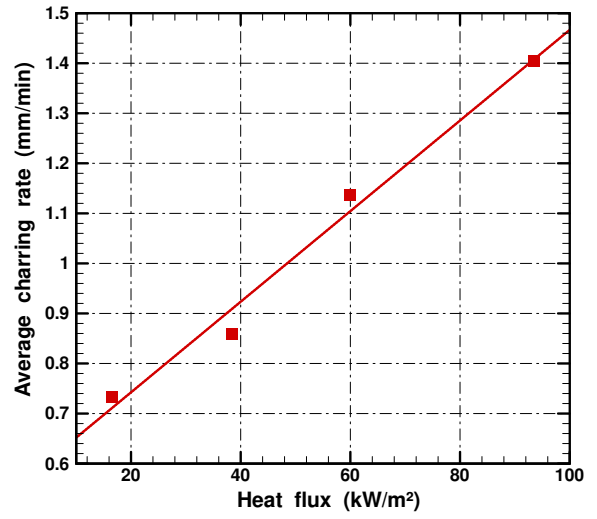
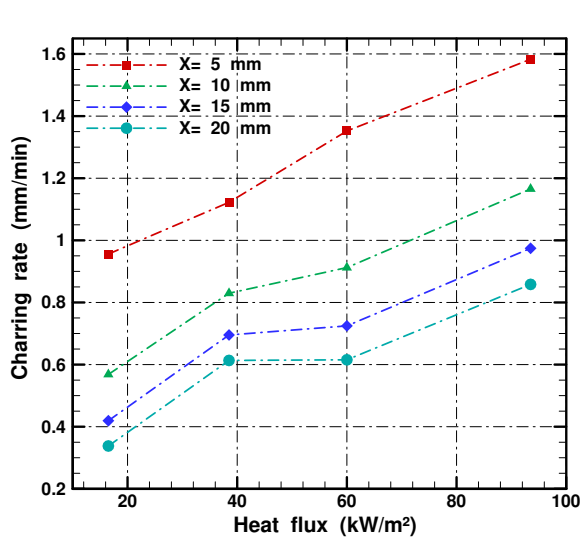


Figure 13: Charring front as a function of time for different heat fluxes. Marks: experimental data – Dot-dashed curves: power law fits – Plain lines: curve tangent at position  $X = 10\text{mm}$ .

The char front location as a function of time for different fluxes is presented in Fig. 13 which also shows the power law fits performed on measurements data. To take into account the delay before the char process begins when the heat flux is small, a power law including a time shift  $t_0$  was chosen according to  $X(t) = a(t - t_0)^b$ ,  $X(t)$  corresponding to the char front position at time  $t$ . For the test performed at  $16.5 \text{ kW}\cdot\text{m}^{-2}$ , two power laws were used - the first for the beginning of the test, before the onset of smouldering combustion and a second after this.

The charring rate was calculated from the analytical derivative of the fits. Given the time shift, comparing the charring rate at a same time for the different heat flux would have no meaning. The charring rate was thus calculated for a fixed position reached by the char front. It is illustrated in Fig. 13 for a position equal to 10 mm (horizontal dashed line). The charring rate at this depth corresponds to the slope of the different curves as represented in the figure. Results are presented in Fig. 14a for depths equal to 5, 10, 15 and 20 mm. As expected, the higher the flux, the higher the charring rate, and the deeper the position, the lower the charring rate. For a given heat flux, as the depth increases, the variation of the charring rate tends to be increasingly lower which is in accordance with the decrease with time of the slope of the rating rate in Fig. 12 (the charring rate tends toward a quasi steady state). The charring rate varies in a linear manner with the incident radiative heat flux, which confirms the findings of Tran and White works [24, 25].



(a) Charring rate as a function of heat flux at different depths. (b) Average (calculated from 0 to 15 mm depth) charring rate as a function of heat flux.

Figure 14: Charring rates for different heat fluxes.

As proposed by Tran and White [24], an average charring rate can be calculated as the depth reached by the char divided by the time needed to reach this depth. Such a calculation was performed with a 15 mm depth. For low heat flux, the time taken into account for this calculation is the time minus the time delay  $t_0$  needed for the charring process to begin. Results are presented in Fig. 14b. A quasi-linear dependence is observed for the average charring calculated in this way.

#### 4. CONCLUSION

In this paper a new technique involving the meticulous implantation of thin wire thermocouples embedded inside wood samples was developed in order to measure the in-depth temperature of wood during its degradation. This was carried out using a specific process, involving cutting the sample, grooving it, setting up the wire thermocouples inside the square-grooves, and reassembling the sample using MUF glue. Numerous thermocouples can be put inside the sample without significantly modifying either the sample thermic or the degradation process. This technique meant the mass loss and the temperature evolution during tests could be measured simultaneously. After setting up the experiment, wood samples were exposed to different heat fluxes from 16.5 to 93.5 kW.m<sup>-2</sup>. For the lowest heat flux, the thermocouple set up permitted us to observe the beginning of smouldering combustion which is particularly visible for measurements made close to the exposed surface. Tests were also performed with sheathed thermocouples placed at 2, 4, 6 and 8 mm in-depth perpendicularly to the isotherm. The results show that significant temperature discrepancies are obtained according to the kind of thermocouple implementation studied. At the same depth and time, the difference between the temperatures measured either by thermocouples perpendicular to the exposed surface or by embedded wire thermocouples parallel to the surface can reach up to 400 °C. Numerical results show that the main reason for this deviation can be attributed to the large heat sink (conductive heat flux) along the thermocouple wire or sheath. This heat sink is found to be greater when the thermocouple or the sheath diameter is large and the thermocouple

is oriented parallel to the conductive heat flux in the sample (*i.e.* perpendicular to isotherms). The deviation may also be explained by the thermal contact resistance between the sample and the thermocouple and by a possible error in the actual position of the thermocouple. The comparison between the char front and the 300 °C isotherm validates the temperature measurement with wire thermocouples. The charring rate derived from the char front increases in a linear manner with the imposed heat flux from 0.5 mm.min<sup>-1</sup> for 16.5 kW.m<sup>-2</sup> to 1 mm.min<sup>-1</sup> for 93.5 kW.m<sup>-2</sup>. In-depth temperatures obtained with the method proposed here are more accurate and reliable than the measurements usually made. This machining made it possible to put thermocouples in the wood sample with the least possible intrusion for temperature measurements. Such reliable data are of primary importance as input for comprehensive models aiming at describing/predicting the thermal degradation of wood.

When possible, putting thermocouples perpendicular to the temperature gradient is by far the preferable solution, and the smaller the thermocouple diameter, the lower the temperature error. Depending on the nature of the samples, this can be done during the manufacture of the samples or otherwise by cutting and gluing. Alternatively, thermocouples can be placed after drilling but perpendicularly to the heat flux. However, this method can lead errors on the position of the thermocouples and cannot be performed for very large panels (long thin drill bits are not available). If putting the thermocouples perpendicular to the heat gradient cannot be done, the use of a thermocouple with a minimum diameter is recommended and the hole should be filled if its diameter is larger than that of the thermocouple.

## ACKNOWLEDGEMENTS

The authors thank the LEMTA's technical staff, Jean-Yves Morel, Sébastien Lejeune, Jérémy Bianchin, Mathieu Weber and Jamal Ouahajjou, for their contribution during samples machining and instrumentation.

## References

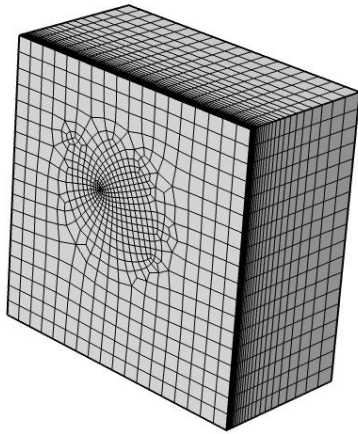
- [1] A. I. Bartlett, R. M. Hadden, and L. A. Bisby, "A review of factors affecting the burning behaviour of wood for application to tall timber construction," *Fire Technology*, vol. 55, no. 1, pp. 1–49, 2019.
- [2] A. Roberts, "Problems associated with the theoretical analysis of the burning of wood," in *Symposium (international) on combustion*, vol. 13, pp. 893–903, Elsevier, 1971.
- [3] Q. Xu, L. Chen, K. A. Harries, F. Zhang, Q. Liu, and J. Feng, "Combustion and charring properties of five common constructional wood species from cone calorimeter tests," *Construction and Building Materials*, vol. 96, pp. 416–427, 2015.
- [4] R. Maciulaitis, D. Lipinskas, and K. Lukosius, "Singularity and importance of determination of wood charring rate in fire investigation," *Materials Science (MEDŽIAGOTYRA)*, vol. 12, pp. 42–47, 2006.
- [5] P. C. R. Collier, *Charring rates of timber*. Building Research Association of New Zealand, 1992.



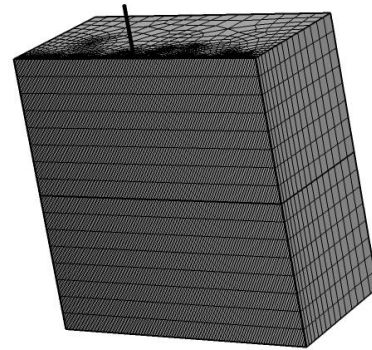
- [6] T. Lie, “Structural fire protection,” American Society of Civil Engineers, 1992.
- [7] Y. Lizhong, G. Zaifu, Z. Yupeng, and F. Weicheng, “The influence of different external heating ways on pyrolysis and spontaneous ignition of some woods,” *Journal of Analytical and Applied Pyrolysis*, vol. 78, no. 1, pp. 40–45, 2007.
- [8] A. Frangi and M. Fontana, “Charring rates and temperature profiles of wood sections,” *Fire and Materials*, vol. 27, no. 2, pp. 91–102, 2003.
- [9] R. H. White and M. A. Dietenberger, “Fire safety,” *Wood handbook: wood as an engineering material. Madison, WI: USDA Forest Service, Forest Products Laboratory, 1999. General technical report FPL; GTR-113: Pages 17.1-17.16*, vol. 113, 1999.
- [10] Y. Lizhong, Z. Yupeng, W. Yafei, and G. Zaifu, “Predicting charring rate of woods exposed to time-increasing and constant heat fluxes,” *Journal of Analytical and Applied Pyrolysis*, vol. 81, no. 1, pp. 1–6, 2008.
- [11] J. M. Njankouo, J.-C. Dotreppe, and J.-M. Franssen, “Experimental study of the charring rate of tropical hardwoods,” *Fire and materials*, vol. 28, no. 1, pp. 15–24, 2004.
- [12] K.-C. Tsai, “Orientation effect on cone calorimeter test results to assess fire hazard of materials,” *Journal of hazardous materials*, vol. 172, no. 2-3, pp. 763–772, 2009.
- [13] S. Wasan, P. Van Hees, and B. Merci, “Study of pyrolysis and upward flame spread on charring materials—part i: Experimental study,” *Fire and Materials*, vol. 35, no. 4, pp. 209–229, 2011.
- [14] J. V. Beck, “Thermocouple temperature disturbances in low conductivity materials,” 1962.
- [15] W. D. Brewer, “Effect of thermocouple wire size and configuration on internal temperature measurements in a charring ablator,” *NASA TN D-3812, National Aeronautics and Space Administration, Langley Research Center, Langley Station, Hampton, Virginia*, 1967.
- [16] P. Reszka and J. Torero, “In-depth temperature measurements in wood exposed to intense radiant energy,” *Experimental Thermal and Fluid Science*, vol. 32, no. 7, pp. 1405–1411, 2008.
- [17] R. Fahrni, J. Schmid, M. Klippel, and A. Frangi, “Correct temperature measurements in fire exposed wood,” in *World Conference on Timber Engineering (WCTE 2018)*, pp. MAT-O9, ETH Zurich, Institute of Structural Engineering (IBK), 2018.
- [18] R. Fahrni, J. Schmid, M. Klippel, and A. Frangi, “Investigation of different temperature measurement designs and installations in timber members as low conductive material,” in *10th International Conference on Structures in Fire (SiF 2018)*, pp. 257–264, Belfast, United Kingdom, 2018.
- [19] Z. Acem, D. Brissinger, A. Collin, G. Parent, P. Boulet, T. H. Y. Quach, B. Batiot, F. Richard, and T. Rogaume, “Surface temperature of carbon composite samples during thermal degradation,” *International Journal of Thermal Sciences*, vol. 112, pp. 427–438, 2017.

- 485 [20] L. Terrei, Z. Acem, V. Georges, P. Lardet, P. Boulet, and G. Parent, “Experimental tools  
486 applied to ignition study of spruce wood under cone calorimeter,” *Fire Safety Journal*, vol. 108,  
487 p. 102845, 2019.
- 488 [21] N. Boonmee and J. Quintiere, “Glowing ignition of wood: the onset of surface combustion,”  
489 *Proceedings of the Combustion Institute*, vol. 30, no. 2, pp. 2303–2310, 2005.
- 490 [22] J. Staggs, “Convection heat transfer in the cone calorimeter,” *Fire Safety Journal*, vol. 44,  
491 no. 4, pp. 469–474, 2009.
- 492 [23] J. Quintiere, “A theoretical basis for flammability properties,” *Fire and Materials: An Inter-  
493 national Journal*, vol. 30, no. 3, pp. 175–214, 2006.
- 494 [24] H. C. Tran and R. H. White, “Burning rate of solid wood measured in a heat release rate  
495 calorimeter,” *Fire and materials*, vol. 16, no. 4, pp. 197–206, 1992.
- 496 [25] R. H. White and H. C. Tran, “Charring rate of wood exposed to a constant heat flux,” in  
497 *Wood and fire safety: 3rd International Scientific Conference: proceedings, May 6-9, 1996,  
498 The High Tatras, Slovak Republic.[Zvolen, Slovak Republic]: Technical University of Zvolen,  
499 Faculty of Wood Technology, 1996.: p. 175-183., 1996.*

## 500 Appendix A. Additional figures with COMSOL modeling



(a) Thermocouple parallel to the heat flux.



(b) Thermocouple perpendicular to the heat flux.

Figure A.15: Sample meshes for COMSOL simulations.